

PROCEDURE FOR DESCRIBING THE DEFORMATION OF MATERIALS TO FRACTURE UNDER CONDITIONS OF NEAR-SUPERPLASTICITY

B. V. Gorev, I. D. Klopotov, and T. É. Zakharova

UDC 539.374+539.376

The ability of metallic materials to deform by hundreds or even thousands of percent, with a substantial drop in resistance to deformation is known as the superplasticity effect.

In [1-6] we demonstrated experimentally for alloys based on titanium, iron, and aluminum that deformation under conditions of near-superplasticity, including a subregion of superplasticity conditions, must be described by taking approaches developed in the theory of creep from the standpoint of the theory of flow. Experimentally substantiated defining equations were proposed for describing the deformation process under arbitrary variation of the stress and temperature without allowance for the third stage of creep. Moreover, the clearly defined length of the stage of secondary creep to fracture is generally observed only near the superplasticity temperature T_s . Outside that range for many alloys the process of deformation before fracture ends with the third (softening) stage of creep.

Below the titanium alloy VT-9 (as-received rod of diameter 16 mm) under pure tension is used as an example to show that the defining equations proposed for the description of creep and creep-rupture strength at a moderate temperature [7] can be extended to the range of temperatures close to superplasticity, $T > 0.6T_{pl}$. The defining equations used have one scalar damageability parameter, which is found by means of the quantities $\omega = \varepsilon/\varepsilon_*$ (ε are instantaneous strains and ε_* are breaking strains). A method is given for determining the parameters of the creep and damageability equations with allowance for tertiary creep over wide ranges of temperature and force.

1. Basic Relations. The defining equations with one scalar damageability parameter q as applied to nonhardening materials for uniaxial deformation in the given temperature range are written as

$$\frac{d\varepsilon}{dt} = \frac{f(\sigma, T)}{(1-q)^{\mu(T)}}, \quad \frac{dq}{dt} = \frac{\Phi(\sigma, T)}{(1-q)^{k(T)}} \quad (0 \leq q \leq 1), \quad (1.1)$$

where the coefficients μ and k of the equations are functions of the temperature.

Assuming that the temperature is a parameter and performing operations similar to those in [7], we transform the system (1.1) into a simpler form, where the softening index in the creep and damageability equations is the same for any temperature. On integrating the second equation of (1.1), we obtain

$$1 - \tau = (1 - q)^{k(T)+1} \quad (0 \leq \tau \leq 1) \quad (1.2)$$

($\tau = (k(T) + 1) \int_0^t \Phi(\sigma, T) dt$ is the normalized time). Next we integrate the first equation of (1.1) for any stressed state with allowance for Eq. (1.2) and we have

$$1 - \omega = (1 - q)^{k(T) - \mu(T) + 1}. \quad (1.3)$$

Here ω is a dimensionless scalar:

Novosibirsk. Translated from *Prikladnaya Mekhanika i Tekhnicheskaya Fizika*, No. 1, pp. 149-157, January-February, 1995. Original article submitted December 29, 1993; revised version submitted March 2, 1994.

$$\omega = (k(T) - \mu(T) + 1) \int_0^t \frac{\Phi(\sigma)}{f(\sigma)} \dot{\varepsilon} dt \quad (0 \leq \omega \leq 1).$$

When the relation obtained is taken into account the system of initial equations reduces to a simpler form,

$$\frac{d\varepsilon}{dt} = \frac{f(\sigma, T)}{(1 - \omega)^{m(T)}}, \quad \frac{d\omega}{dt} = \frac{\varphi(\sigma, T)}{(1 - \omega)^{m(T)}} \quad (0 \leq \omega \leq 1), \quad (1.4)$$

where $\varphi(\sigma, T) = (k - \mu + 1)\Phi(\sigma, T)$; $m(T) = \mu/(k - \mu + 1)$.

From (1.2) and (1.3), with allowance for the notation (1.4) introduced, we have the equation

$$(1 - \omega)^{m(T)+1} = 1 - \tau, \quad (1.5)$$

which in the normalized coordinates $\omega - \tau$ represents the equation of a single curve for each fixed temperature [7].

System (1.1) is not equivalent to system (1.4), since it contains an extra parameter. The value of k in system (1.1) cannot be determined independently and so there is some arbitrariness. It can be removed by endowing q with a physical meaning or by means of some other propositions. However, since ω is a function of the initial damageability parameter q and varies within the same limits, from the phenomenological standpoint we assess the damageability of the material from ω and, without loss of generality, we henceforth assign it the sense of the damageability parameter.

The resulting system of defining equations (1.4) with the same softening functions $m(T)$ in both equations relates ω with the values of ε and ε_* measured in uniaxial steady-state experiments; the fracture strains depend arbitrarily on the stresses and temperature [$\varepsilon_* = \varepsilon_*(\sigma, T)$].

Integrating system (1.4) for steady-state conditions ($T = \text{const}$, $\sigma = \text{const}$), we find

$$\begin{aligned} \omega &= 1 - [1 - (m + 1)\varphi(\sigma, T)t]^{1/(m+1)}, \quad \varepsilon = \frac{f(\sigma, T)}{\varphi(\sigma, T)}\omega, \\ \omega &= \varepsilon/\varepsilon_*, \quad \varepsilon_* = f(\sigma, T)/\varphi(\sigma, T), \\ \tau &= t/t_*, \quad t_* = \frac{1}{(m + 1)\varphi(\sigma, T)}. \end{aligned} \quad (1.6)$$

Hence in this case the damageability parameter is equal to the ratio of the instantaneous strain to the fracture strain $\omega = \varepsilon/\varepsilon_*$ ($\varepsilon_* \neq \text{const}$), the normalized time is the ratio of the current time to the time to fracture $\tau = t/t_*$. The possibility of correctly using the defining equations in the form (1.4) will verify the single-curve equation (1.5) at a fixed temperature in the relative coordinates $\omega - \tau$. In other words, following the single-curve equation, it is necessary to check the similarity of the initial curves of deformation to fracture in terms of the damageability of the material and time.

In Figs. 1-3 points in the form of diagrams of $\varepsilon = \varepsilon(t)$ represent the experimental data from tensile tests with $\sigma = \text{const}$ for various temperatures in the interval from 700 to 1000°C (the values of the fracture strains are indicated by asterisks). Bearing in mind that the elastic strain at those temperatures is $\varepsilon < 0.5\%$ [1, 9], we incorporated it into the irreversible creep deformation when plotting the strain curves with developed strains (more than several per cent). The logarithmic strains were used to calculate the final strains. The stresses in the experiments were kept constant up to fracture by adjusting the load on the basis of the complete incompressibility of the material under developed [8] and large strains [9, p. 75] (the area of the specimen and the corresponding load were calculated for every 0.5-1% of strain). In the tests we used cylindrical specimens having a diameter of 7 mm and a "short" effective length of 40 mm. The elongation of the specimen with time was charted by a recorder, using POS and IKZ potentiometric transducers, which were mounted on the outside of the furnace by means of an extensometer. In all the experiments the specimens were heated for less than 1 h before the load was applied. The fracture strain ε_* varies randomly as a function of the stress and temperature, but is almost constant at each fixed temperature in an interval of up to 4 h and the maximum of its values obtained for various $\sigma_n = \text{const}$ rises with the temperature, from $\varepsilon_* \approx 0.5$ at 700°C to $\varepsilon_* \approx 2$ at 1000°C, but decreases at temperatures above 1000°C. Thus, the maximum ε_* at 1050°C is of the order of 1.6.

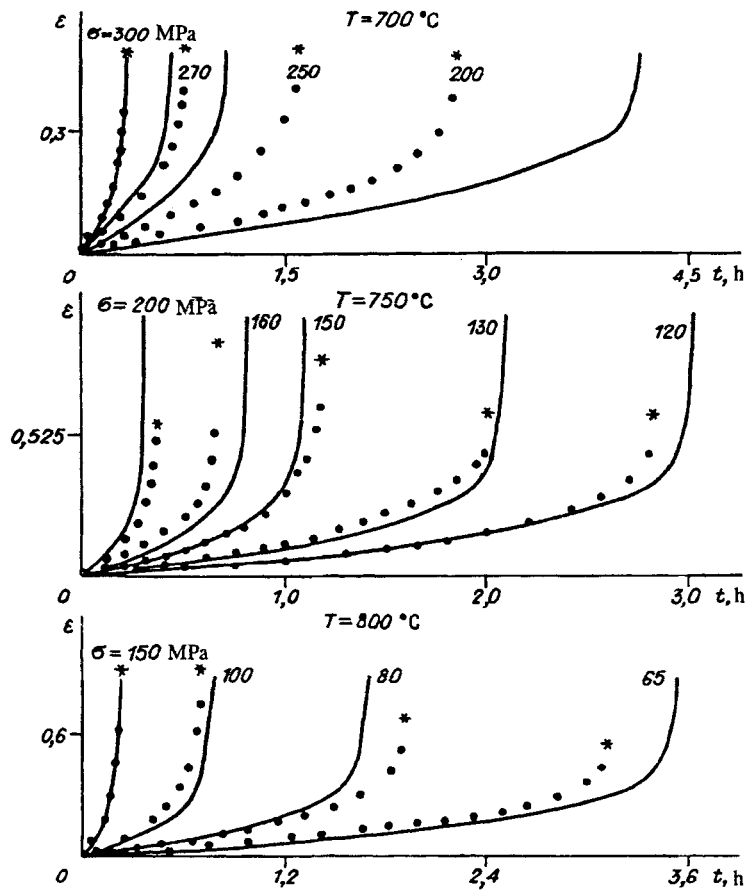


Fig. 1

Figure 4 shows the same experimental data as in Figs. 1-3, but converted to the reduced coordinates $\omega = \varepsilon/\varepsilon_*$, $\tau = t/t_*$ (the temperature is given for the respective diagrams): a) $\sigma = 8, 10, 11.5, 200, 250,$ and 300 MPa (points 1-6); b) $\sigma = 10, 12, 15, 120, 130,$ and 200 MPa (points 1-6); c) $\sigma = 65, 80, 100,$ and 150 MPa (points 1-4); d) $\sigma = 37, 45, 50,$ and 70 MPa (points 1-4); e) $\sigma = 14, 15, 18,$ and 22 MPa (points 1-4). The initial strain curves so plotted are grouped together as a dense bundle into one curve for each temperature considered, thus supporting the notation of the damageability equation in the form of the state equation (1.4) and also supporting the hypothesis of a single curve for a fixed temperature (1.5).

The slowest rate of damage buildup is observed in the temperature interval $980-1000^\circ\text{C}$. In this range creep is subordinate to steady-state flow up to fracture, with the largest deformations occurring at the time of the fracture. The given characteristic temperature interval evidently is optimal for uniaxial deformation processes and coincides with the region of optimal temperature T_s (from the standpoint of continuum mechanics deformation according to the laws of viscous flow can be assumed to be the principal feature of the superplasticity mode).

2. Determination of the Parameters of the Creep and Damageability Equations. With allowance for the experimental substantiation of the damageability equation in the form (1.4) and the expression of the damageability parameter in terms of the experimentally determined quantity $\omega = \varepsilon/\varepsilon_*$ we indicate a method of determining the coefficients of the equations at constant temperature. Assuming that those coefficients depend on both the temperature and the parameter, we can easily obtain the functional relations in the range of temperatures from the experimental data in Figs. 1-4.

The softening index m_i in Eq. (1.4) at a fixed temperature T_i is found by (1.5) from the slope of the straight line $\ln(1 - \tau) = (m + 1)\ln(1 - \omega)$ as the mean square of m_n for various $\sigma_n = \text{const}$. The function $\varphi(\sigma, T_i)$ from (1.6) is chosen on the basis of the best approximation of the time to fracture as a function of the stress by the σ - t_* experimental curve:

$$\varphi(\sigma, T_i) = [(m_i + 1)t_*(\sigma, T_i)]^{-1}. \quad (2.1)$$

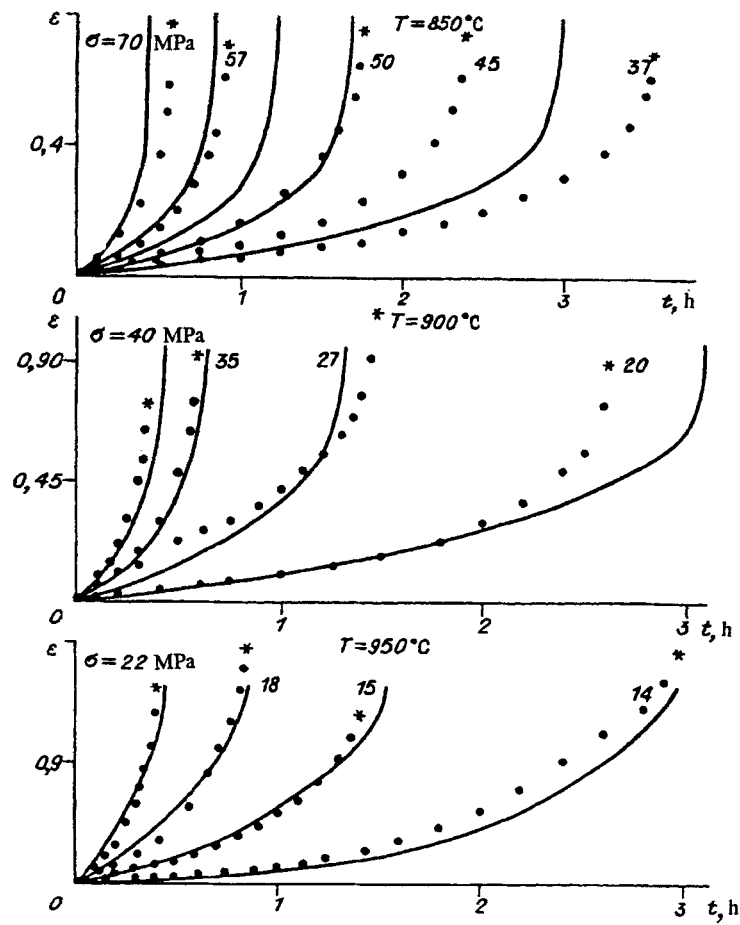


Fig. 2

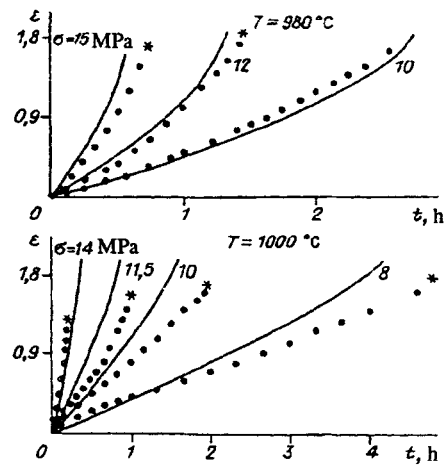


Fig. 3

The function $f(\sigma, T_i)$ is determined from (1.6) and has the same form as does the function φ if $\varepsilon(\sigma, T_i)$ is a monotonic function:

$$f(\sigma, T_i) = \varepsilon_*(\sigma, T_i) \varphi(\sigma, T_i). \quad (2.2)$$

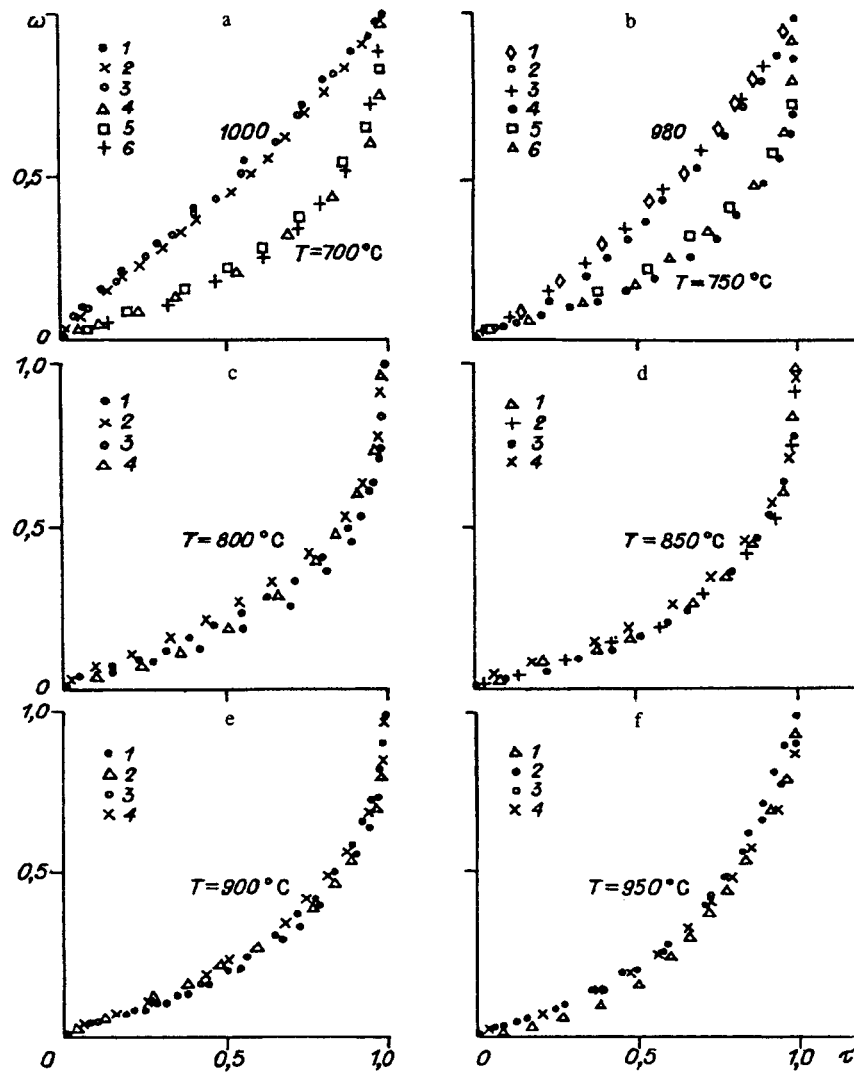


Fig. 4

The most common relations describing constant-temperature creep processes in materials are :

$$f(\sigma) = B_1 \sigma^n, f(\sigma) = B_2 \exp(\alpha \sigma) \quad (2.3)$$

(B_1 , B_2 , and α are material characteristics). These characteristics are assumed to be functions of the temperature if the problem is to describe creep processes over a range of temperatures.

The above relations work satisfactorily only for high stresses and short times to fracture. Inclusion of low stresses requires more complicated relations, e.g., [4]

$$f(\sigma, T) = \exp \Phi(\sigma, T) \quad (\Phi(\sigma, T) = \sum_{k=-n}^{k=m} \alpha_k \sigma^k). \quad (2.4)$$

Each coefficient α_k is in turn assumed to depend on the temperature. Finally, exp is taken to mean either a parabolic or hyperbolic dependence on the temperature. A program has been developed for computer processing of experimental data with automatic selection of the approximation functions from Eqs. (2.3) and (2.4). The computer selects the relation that best describes the experimental data. Once the function has been determined, the temperature coefficients that appear in it are approximated by the procedure described below.

TABLE 1

i	n_i	m_i	K_i	B_i
0	$8,05730 \cdot 10^1$	$-2,5447147 \cdot 10^3$	$-8,7995845 \cdot 10^2$	$-2,270629 \cdot 10^3$
1	$-1,7628 \cdot 10^{-1}$	$1,1410843 \cdot 10^1$	2,597382	9,110224
2	$1,0 \cdot 10^{-4}$	$-1,9025853 \cdot 10^{-2}$	$-2,6964759 \cdot 10^{-3}$	$-1,4069883 \cdot 10^{-2}$
3	—	$1,4016815 \cdot 10^{-5}$	$1,0598977 \cdot 10^{-6}$	$9,8341378 \cdot 10^{-6}$
4	—	$-3,8568588 \cdot 10^{-9}$	$-9,9599535 \cdot 10^{-11}$	$-2,6219111 \cdot 10^{-9}$

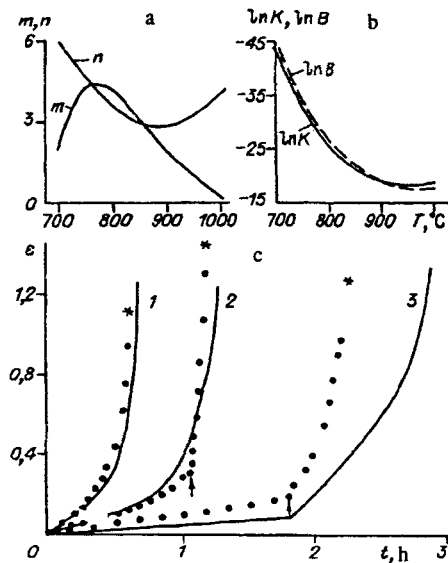


Fig. 5

For the alloy VT-9 in the range of temperatures studied (700-1000°C) and a time of less than 4 h to fracture Eq. (2.1) best describes the power-law dependence $\varphi(\sigma, T) = K(T)\sigma^{n(T)}$. For each fixed temperature the fracture strain was assumed to be constant ($\varepsilon_* = \text{const}$) and equal to the maximum of the values obtained for various $\sigma_n = \text{const}$. From (2.2) it follows that

$$f(\sigma, T) = B(T)\sigma^{n(T)}, \varepsilon_* = B(T) / K(T).$$

For VT-9 Eqs. (1.4) are written as

$$\frac{d\varepsilon}{dt} = \frac{B(T)\sigma^{n(T)}}{(1 - \omega)^{m(T)}}, \frac{d\omega}{dt} = \frac{K(T)\sigma^{n(T)}}{(1 - \omega)^{m(T)}}. \quad (2.5)$$

All the coefficients in (2.5) determined for each fixed temperature were then approximated on a computer for the entire temperature range. The coefficients m and n in the temperature dependences were approximated by the polynomials

$$n = \sum_{i=0}^{i=a} n_i T^i, \quad m = \sum_{i=0}^{i=b} m_i T^i. \quad (2.6)$$

The coefficients K and B were approximated by

$$K = \exp\left(\sum_{i=0}^{i=c} K_i T^i\right), \quad B = \exp\left(\sum_{i=0}^{i=d} B_i T^i\right). \quad (2.7)$$

The maximum degrees of the polynomials were chosen for the best possible description of the experimental values of $n(T)$, $m(T)$, $\ln K(T)$, and $\ln B(T)$ in the given temperature range for the minimum values of those degrees. We obtained the values $a = 2$ and $b = c = d = 4$. The coefficients in relations (2.6) and (2.7) were determined by solving the system of linear equations

$$\begin{aligned} n(T_j) &= \sum_{i=0}^{i=2} n_i T_j^i, & m(T_j) &= \sum_{i=0}^{i=4} m_i T_j^i, \\ \ln K(T_j) &= \sum_{i=0}^{i=4} K_i T_j^i, & \ln B(T_j) &= \sum_{i=0}^{i=4} B_i T_j^i. \end{aligned}$$

The coefficients so obtained (Table 1) were used to determine all the constants in Eq. (2.5). As an illustration Figs. 5a, b give the calculated values of $n(T)$, $m(T)$, $\ln B(T)$, and $\ln K(T)$ as a function of the temperature. In Figs. 1-3 lines show the calculations from the characteristics obtained in the temperature range 700-1000°C. Figure 5c shows the experimental points and the calculated lines, which describe experiments with overloads; arrows indicate the overload time and asterisks indicate the time to fracture; 1) experiment at 700°C and $\sigma = 300$ MPa, during which the specimen was overloaded to $\sigma = 18$ MPa and at 950°C (the time taken to heat the specimen to 950°C was not included in the duration of the entire experiment), 2) a similar experiment at $T = 750^\circ\text{C}$ and $\sigma = 150$ MPa with an overload at $T = 950^\circ\text{C}$, $\sigma = 18$ MPa, overload time 1.05 h, and 3) an experiment at $T = 700^\circ\text{C}$ and $\sigma = 200$ MPa with an overload at $T = 950^\circ\text{C}$, $\sigma = 15$ MPa, overload time 1.8 h.

The fully satisfactory agreement between the calculated and experimental data suggests that defining equations with one scalar damageability parameter can be used to describe the process of deformation under near-superplastic conditions for materials in which the strain fracture depends significantly on the temperature. Experiments in the temperature range from 700 to 1000°C for the alloy studied demonstrated that the initial strain curves at a fixed temperature in coordinates of material damageability vs time ($\omega = \varepsilon/\varepsilon_*$, t) are similar, whereby the notation of the damageability equation in the form $d\omega/dt = \varphi(\sigma, T)\psi(\omega, T)$.

The determination of the damageability parameter by means of measurements in a uniaxial experiment indicates that the results of experiments can be approximated and extrapolated on the basis of a description with single analytical relations over a wide range of temperatures and forces and a single method can be given determining the functional relations with allowance for the softening of the material.

It has been determined that the lowest rate of damage build-up is observed in the titanium alloy VT-9 in the region of the optimal superplasticity temperature ($T_s = 980\text{-}1000^\circ\text{C}$); in this case creep is subordinate to steady-state flow to fracture and the largest strains occur at fracture.

The work was done with financial support from the Russian Fund for Basic Research (Project 93-0132-16506).

REFERENCES

1. B. V. Gorev, A. A. Ratnichkin, and O. V. Sosnin, "Laws of deformation of materials under near-superplasticity conditions. Communication 1. Uniaxial stressed state," *Prob. Proch.*, No. 11 (1987).
2. B. V. Gorev, A. A. Ratnichkin, and O. V. Sosnin, "Laws of deformation of materials under near-superplasticity conditions. Communication 2. Plane Stress State," *Prob. Proch.*, No. 11 (1987).
3. O. V. Sosnin, B. V. Gorev, and A. A. Ratnichkin, "Pressure shaping of materials under creep and superplasticity conditions," *Izv. Sib. Otd. Akad. Nauk SSSR. Ser. Tekh. Nauk*, No. 11, No. 3 (1987).
4. O. V. Sosnin, B. V. Gorev, and A. A. Ratnichkin, "Laws of deformation of metals under near-plasticity conditions," in: *Problems of Nonlinear Mechanics of a Deformed Bodies* [in Russian], Sverdlovsk (1990).
5. O. V. Sosnin, B. V. Gorev, and A. A. Ratnichkin, "Mechanics of deformation of material under near-plasticity conditions," in: *Current Problems of the Mechanics of a Deformable Body* [in Russian], *Izv. Akad. Nauk Resp. Kaz.*, Alma-Ata (1992).
6. O. V. Sosnin, B. V. Gorev, and A. A. Ratnichkin, "Mechanics of superplasticity and its relation to high-temperature creep," *Sib. Fiz.-Tekh. Zh.*, No. 4 (1993).

7. B. V. Gorev and I. D. Klopotov, "Description of creep and long-term strength by equations with one scalar damageability parameter," *Prikl. Mekh. Tekh. Fiz.*, No. 5 (1994).
8. V. V. Rubanov, "Verification of the hypothesis of incompressibility by experiments on the aluminum alloy AK4-1T," in: *Dynamics of Continuous Media* [in Russian], No. 75, Akad. Nauk SSSR, Sib. Otd., Inst. Gidrodinamiki (1986).
9. K. I. Romanov, *Mechanics of Hot Deformation of Metals* [in Russian], Mashinostroenie, Moscow (1993).